European Radiology (2019) 29:3854–3861
https://doi.org/10.1007/s00330-019-06051-9

PAEDIATRIC

The value of non-invasive vascular elastography (NIVE) in detecting early vascular changes in overweight and obese children

Ramy El Jalbout[1] · Guy Cloutier[2] · Marie-Hélène Roy-Cardinal[2] · Mélanie Henderson[3] · Emile Levy[3] · Chantale Lapierre[1] · Gilles Soulez[4] · Josée Dubois[1]

Received: 11 September 2018 / Revised: 3 January 2019 / Accepted: 30 January 2019 / Published online: 7 March 2019

Abstract

Objectives Evaluate non-invasive vascular elastography (NIVE) in detecting vascular changes associated with obese children.

Methods Case-control study to evaluate NIVE in 120 children, 60 with elevated body mass index (BMI) (≥ 85th percentile for age and sex). Participants were randomly selected from a longitudinal cohort, evaluating consequences of obesity in healthy children with one obese parent. Radiofrequency ultrasound videos of the common carotid artery were obtained. The carotid wall was segmented and NIVE applied to measure cumulated axial strain (CAS), cumulated axial translation (CAT), cumulated lateral translation (CLT), maximal shear strain (Max |SSE|), and intima-media thickness (IMT). Multivariate analyses were used controlling for age, sex, Tanner stage, blood pressure, and low-density lipoprotein. Statistical significance was set to 0.05–0.008. Participants were 10–13 years old (mean 11.4 and 12.0, for normal and elevated BMI groups, $p < 0.001$), 58% and 63% boys, respectively. Groups differed in age, Tanner stage, and blood pressure. In the normal BMI group, there was weak correlation between systolic blood pressure and Max |SSE| ($r = 0.316$, $p = 0.01$) and weak correlation between pulse pressure and Max |SSE| ($r = 0.259$, $p = 0.045$). After Bonferroni correction, CAT was significantly higher in the elevated BMI group (0.68 ± 0.24 mm vs. 0.52 ± 0.18 mm), $p < 0.001$. CAS/CAT was significantly lower in the elevated BMI group (9.54 ± 4.8 vs. 13.34 ± 6.46), $p = 0.001$. IMT was significantly higher in the elevated BMI group (0.36 ± 0.05 mm vs. 0.32 ± 0.05 mm) before Bonferroni correction, $p = 0.013$.

Conclusions NIVE detected differences in CAT and CAS/CAT in elevated BMI children. NIVE is a promising technique to monitor radiological markers of subclinical atherosclerosis.

Key Points

- *NIVE is a non-invasive technique based on measurement of subsegmental focal deformation of vascular wall to detect subclinical changes in arterial wall compliance.*
- *Children with elevated BMI showed increased carotid artery wall movement during systole, as compared to normal BMI children (mean 0.68 ± 0.24 mm vs. 0.52 ± 0.18 mm; $p < 0.001$) and a lower ratio of vascular wall strain to wall movement during systole (mean 9.54 ± 4.8 vs. 13.34 ± 6.46; $p = 0.001$).*
- *The detection of these subclinical changes helps physicians in the stratification of children at risk of atherosclerosis and guides in the implementation of preventive measures.*

Keywords Intima-media thickness · Ultrasound · Cardiovascular diseases · Obesity · Children

✉ Ramy El Jalbout
ramy.el-jalbout.hsj@ssss.gouv.qc.ca

[1] Department of Radiology, Sainte Justine Hospital, University of Montreal, 3175 Cote-Sainte-Catherine Road, Montreal, Quebec H3T 1C5, Canada

[2] Laboratory of Biorheology and Medical Ultrasonics, University of Montreal Hospital Research Centre (CRCHUM), Montreal, Quebec, Canada

[3] Department of Pediatrics, Sainte Justine Hospital, University of Montreal, Montreal, Quebec, Canada

[4] Department of Radiology, University of Montreal Hospital (CHUM), Montreal, Quebec, Canada

Abbreviations

ANOVA	Analysis of variance
BMI	Body mass index
CAS	Cumulated axial strain
CAT	Cumulated axial translation
CLT	Cumulated lateral translation
IMT	Intima-media thickness
LDL	Low-density lipoprotein
Max |SSE|	Maximal shear strain
NIVE	Non-invasive vascular elastography
PWV	Pulse wave velocity
RF	Radiofrequency

Introduction

Atherosclerosis begins subclinically in childhood [1, 2], particularly in children with obesity [3, 4]. The initial step is endothelial dysfunction, followed by abnormal vasomotion and increased arterial stiffness [5]. Fat deposition, combined with changes in the mechanical properties of the carotid wall, ultimately leads to atherosclerotic plaques in adulthood [6].

There are several methods to assess subclinical changes in vessel wall compliance [7, 8]. Carotid artery intima-media thickness (IMT) is a marker associated with early atherosclerosis, but in the pediatric population, it varies according to technique [9–12]. Pulse wave velocity (PWV) is currently the method of choice to assess arterial stiffness clinically [13]. PWV refers to the time of propagation of the arterial pulse pressure. The beta stiffness index (β), or the difference in luminal diameter between systole and diastole, is another indicator of arterial wall elasticity [8].

Non-invasive vascular elastography (NIVE) makes use of the natural cardiac pulse to evaluate vessel wall biomechanics. Compared to PWV and the β-stiffness index providing a global measure of the vessel wall elasticity, NIVE assesses a local deformation of the vessel wall displayed on two-dimensional images [14]. Elastogram parameters are averaged over the vessel wall at each time frame to provide time-varying curves representing the vessel wall deformation and translation during the whole cardiac cycle [14–16].

NIVE is a promising non-invasive alternative to elasticity and IMT measurement, with proven reliability in adults [17, 18]. The aim of this study was to evaluate the potential of NIVE as a non-invasive method to calculate IMT and detect early changes in vascular biomechanics associated with obesity in children.

Materials and methods

Study design and patient population

We conducted a case-control observational prospective study comparing NIVE parameters in children with normal and elevated body mass index (BMI). We randomly selected 60 overweight/obese children (as defined by BMI ≥ the 85th percentile for age and sex) and 60 non-overweight children (BMI < 85th percentile) from a longitudinal cohort evaluating the cardiometabolic consequences of obesity in childhood [19, 20]. IMT and other measures analyzed for the present study were taken at the second visit of the cohort, in 2008–2011. Recruitment pamphlets for the original cohort were distributed in schools. Inclusion criteria were the following: age 8–10 years at cohort entry, Caucasian origin, healthy status and not known hypercholesterolemic, and having at least one obese parent (as defined by BMI ≥ 30 kg/m^2) irrespective of other co-morbidities. Exclusion criteria were the following: cognitive impairment, use of hypertensive medication or oral steroids, maternal status either pregnant or breastfeeding, or geographical location subject to change. The duration of overweight and obesity is not available for this initial assessment. The study was approved by applicable institutional ethics review boards. Written informed consent was obtained from the children's caregivers.

Outcome measures

Primary endpoints were cumulated axial strain (CAS), cumulated axial translation (CAT), CAS/CAT, cumulated lateral translation (CLT), and maximal shear strain (Max |SSE|). The secondary endpoint was IMT, calculated using the same video as the other NIVE analyses. Since obesity and lipid profiles are associated with cardiovascular disease, and since NIVE reflects the inherent deformation of the vessel wall secondary to distension and relaxation in systole and diastole, we included the following as independent variables: BMI, age, sex, systolic and diastolic blood pressures (taking into account pulse pressure), and low-density lipoprotein (LDL). All information and carotid ultrasound data were collected at the same visit. Blood pressure was taken 1.5 hours on average before the ultrasound exam. Weight was measured twice on an electronic scale to the nearest 0.1 kg. Height was measured twice to the nearest 0.1 cm. BMI was calculated as weight (kg)/height (m)^2. We defined overweight and obesity according to the definition used by the Centers for Disease Control, with *z*-scores adjusted for age and sex. Tanner stage was determined by specialized staff. Blood pressure was calculated as the mean of the last three of five measures taken one minute apart after at least five minutes of rest, using a Dinamap XL Vital Signs Monitor. Serum LDL was measured after overnight fasting.

Image acquisition

We acquired ultrasound images of the far wall of the common carotid artery, as recommended by the Mannheim consensus, using a transcutaneous ultrasound probe within 2 cm from the carotid bifurcation in longitudinal view. The participants were in the supine position with the head tilted 45° to the opposite side. We used a linear array L10-5 40-mm ultrasound transducer (model 410503) on the MyLab70 platform (Esaote) equipped with an ART.LAB application (Pie Medical Equipment B.V.) to record a radiofrequency (RF) digital data stream which typically included 250 to 300 images. All participants had more than one video sequence recorded. Some had videos done by two independent operators with more than five years of experience in ultrasound. Analysis of the time sequence videos was blinded as to participant group and was done by a research assistant (MHRC) with 8-year experience in NIVE.

Carotid wall segmentation and NIVE computation

Segmentation of the vessel wall and NIVE computation were performed for the entire cine-loop acquisition using a software implemented in a dedicated platform (ORS Visual, Object Research Systems (ORS) Inc.). A region of interest delineated by two contours defining the lumen-intima and the media-adventitia interfaces was manually traced on a single frame of the cine-loop acquisition. These contours were then automatically adapted according to gray level Nakagami probability distribution modeling, and propagated to segment the carotid artery wall on all remaining frames [21, 22]. Non-invasive elastography was then applied to the segmented area to generate 2D displacement maps between consecutive ultrasound frames. Elastography provided axial and lateral translations, strain and shear strain (axial and lateral indicate respectively the directions along and perpendicular to the ultrasound beam). Translations are rigid displacements within the cardiac cycle. The axial strain indicates a compression or dilation of the vessel wall produced by the pulsating blood pressure. The shear strain corresponds to an angular deformation due to the mechanical heterogeneity of the vessel wall. Two-dimensional displacement images were computed using local overlapping measurement windows of size 6.3×0.9 mm^2 (20×40 pixels); pixels within the window but outside the segmented carotid artery wall were excluded from estimation (Fig. 1).

CAS, as a percentage, measures the range of variation in axial strain within a cardiac cycle. CAT, in millimeters, reflects the total amplitude of the axial translation of the vessel wall as it distends. CAS/CAT indicates strain per unit axial translation. Max |SSE|, as a percentage, is the peak axial shear strain during a cardiac cycle. CLT, in millimeters, represents the total amplitude of the movement from left to right in a longitudinal view of the carotid artery. IMT was calculated from the automatically detected contours and was averaged along the entire segmented vessel wall and over the entire length of the cine-loop (more than one cardiac cycle), excluding the adventitia. Each outcome was averaged over all available cardiac cycles.

Statistical analysis

Taking into consideration the variables we wished to include in the study, we prospectively calculated a sample size of 90 participants to achieve a power of 80% for a significance level of $p < 0.05$. We used univariate unpaired two-tailed Student's t test and chi-square analyses to compare demographic, clinical, and biological variables between the normal weight and overweight/obese groups. We also assessed correlations between systolic and diastolic pulse pressure and the four NIVE parameters and IMT, using Pearson's correlation coefficient. $P < 0.05$ indicated statistical significance throughout. All categorical and linear variables were included in a

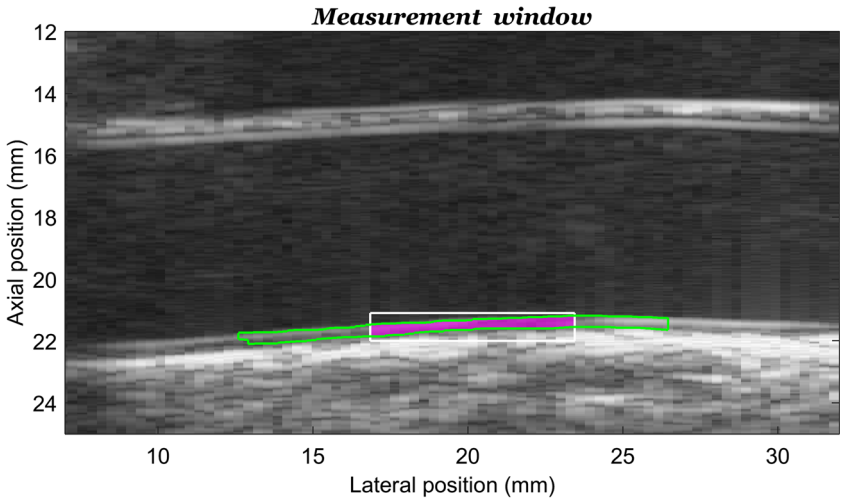

Fig. 1 Example of a measurement window shown on a static image of the common carotid artery. The segmented wall region and measurement window are the green line and white rectangle, respectively. Pixels within both the segmented wall and measurement window (magenta region) were used to compute the two-dimensional displacements corresponding to the window center point

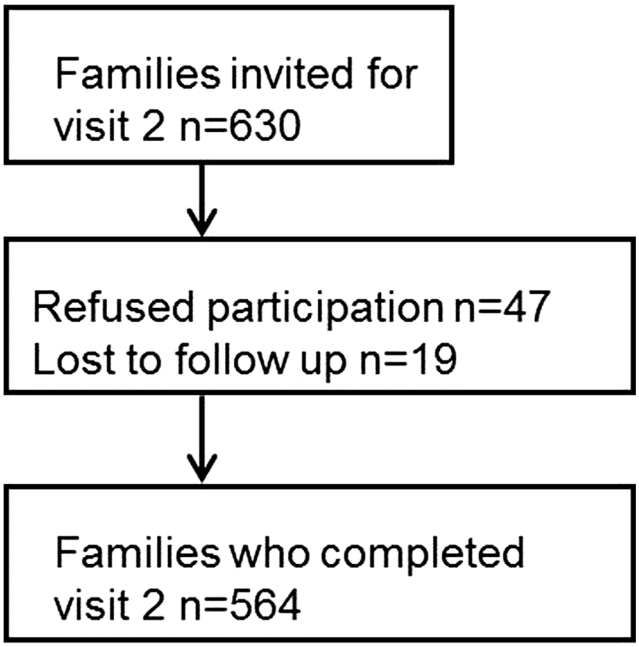

Fig. 2 Flow chart of the visit from which 120 children were randomly selected for NIVE assessment, $n = 60$ in each group

multivariate model (ANOVA) while controlling for age, sex, Tanner stage, blood pressure, and LDL. We applied Bonferroni correction to confidence intervals as well. The reproducibility of the elastography parameters was evaluated by an interobserver agreement analysis in 18 patients who had two video sequences for the same side performed by two independent operators. A two-way ANOVA analysis was done for the 120 participants for the correlation between weight group and operator for all the NIVE-derived measures. All analyses were performed using SAS version 9.3 and MedCalc version 17.2.

Results

A flow chart of the cohort from which the two groups were obtained is shown in Fig. 2. Demographic and social profiles have been previously described [19]. Of the 120 randomly selected children, 35 (58%) and 38 (63%) were boys, in the normal and elevated BMI groups, respectively (Table 1). Mean age (95% confidence interval) was slightly older in the elevated BMI group as compared to normal BMI group (12.0 years (11.8–12.2) vs. 11.4 years (11.2–11.7), respectively; $p < 0.001$). The two groups also differed significantly with respect to LDL, systolic and diastolic blood pressure, and Tanner stage. Three children in the normal BMI group had borderline high LDL blood levels while one child in the elevated BMI group had borderline LDL and another had high LDL; the remainder had acceptable levels, as per American Academy of Pediatrics standards (< 2.85 mmol/L). Only one child had high systolic blood pressure, defined as > 95th percentile for age and sex, and that was in the elevated BMI group. There were 26 children (43%) with Tanner stage ≥ 2 in the normal BMI group and 43 (72%) in the elevated BMI group.

Pearson correlation analysis did not show any relationship between blood pressure and NIVE-derived measures and IMT in the elevated BMI group (Table 2). In the normal BMI group, there was a weak correlation between systolic blood pressure and Max |SSE| ($r = 0.316$, $p = 0.013$). There was also a weak correlation between pulse pressure and Max |SSE| ($r = 0.259$, $p = 0.045$) (Table 2). There was no collinearity between blood pressure and outcomes.

ANOVA multiple comparisons for primary outcome variables were done between groups and adjusted for age, sex, Tanner stage, blood pressure, and LDL. After Bonferroni

Table 1 Group comparison of BMI *z*-score, age, sex, Tanner stage, blood pressure, and LDL

	Normal BMI group ($n = 60$)	Elevated BMI group ($n = 60$)	*p* value
BMI *z*-score, mean (95% CI)	− 0.73 (− 0.92; − 0.54)	1.96 (1.83; 2.08)	< 0.001
Age (years), mean (95% CI)	11.4 (11.2; 11.7)	12.0 (11.8; 12.2)	< 0.001
Sex male, *n* (%)	35 (58)	38 (63)	0.70
Tanner stage, *n* (%)			
1	34 (57)	17 (28)	0.007
2	17 (28)	18 (30)	
3	6 (10)	16 (27)	
4	3 (5)	7 (12)	
5	0 (0)	2 (3)	
Systolic blood (mmHg), mean (95% CI)	93 (91; 95)	100 (97; 103)	< 0.001
Diastolic blood pressure (mmHg), mean (95% CI)	48 (46; 49)	52 (50; 54)	< 0.001
LDL (mmol/L), mean (95% CI)	2.14 (2.00; 2.27)	2.36 (2.20; 2.53)	0.033

Threshold of statistical significance set at $p < 0.05$

BMI body mass index

Table 2 Pearson correlation coefficients and *p* values for blood pressure and outcomes in both groups of children with normal and elevated BMI

	CAS		CAT		CLT		|SSE|	
	Normal BMI	Elevated BMI	Normal BMI	Elevated BMI	Normal BMI	Elevated BMI	Normal BMI	Elevated BMI
Systolic blood pressure	$r = 0.008$ $p = 0.94$	$r = 0.111$ $p = 0.40$	$r = 0.057$ $p = 0.66$	$r = 0.112$ $p = 0.39$	$r = 0.158$ $p = 0.23$	$r = -0.042$ $p = 0.74$	$r = 0.316$ $p = 0.013$	$r = 0.116$ $p = 0.37$
Diastolic blood pressure	$r = 0.062$ $p = 0.63$	$r = -0.166$ $p = 0.20$	$r = -0.167$ $p = 0.19$	$r = 0.097$ $p = 0.45$	$r = 0.077$ $p = 0.56$	$r = -0.042$ $p = 0.75$	$r = 0.147$ $p = 0.25$	$r = 0.016$ $p = 0.90$
Pulse pressure	$r = -0.039$ $p = 0.76$	$r = 0.240$ $p = 0.06$	$r = 0.202$ $p = 0.12$	$r = 0.174$ $p = 0.18$	$r = 0.127$ $p = 0.33$	$r = 0.00$ $p = 0.99$	$r = 0.259$ $p = 0.045$	$r = -0.018$ $p = 0.88$

BMI body mass index, *CAS* cumulated axial strain, *CAT* cumulated axial translation, *CLT* cumulated lateral translation, *|SSE|* maximal shear strain

correction, only CAT and CAS/CAT remained significant between groups, with a lower CAT and a correspondingly higher CAS/CAT ratio in the normal BMI group as compared to the elevated BMI group (Table 3). Using unadjusted values, Max |SSE| was also significantly lower in the normal BMI group (0.48% vs. 0.53% for normal and elevated BMI groups, respectively; $p = 0.04$). Figure 3 shows NIVE curves for the same parameters.

IMT was significantly lower in the normal BMI group as compared to the elevated BMI group (0.32 mm vs. 0.36 mm, respectively), with an adjusted mean difference of 0.03 (95% CI 0.007–0.054, $p = 0.013$), before Bonferroni correction. After Bonferroni correction, however, this was no longer significant (Table 3). There was no correlation between IMT and CAT in either group ($r = 0.177$, $p = 0.17$ in the normal BMI group and $r = 0.088$, $p = 0.50$ in the elevated BMI group).

The intraclass correlation coefficient (ICC) was good for CAT (0.61), fair for CAS/CAT (0.55), CLT (0.42), Max |SSE| (0.42), and NIVE-derived IMT (0.52). ICC was weak for CAS (0.19). The two-way ANOVA analysis did not show correlation between group category (normal versus elevated BMI) and operator for all the NIVE-derived measures (CAS $p = 0.51$, CAT $p = 0.64$, CAS/CAT $p = 0.13$, CLT $p = 0.76$, Max |SSE| $p = 0.56$) and for IMT ($p = 0.93$).

Discussion

NIVE measurements were able to discern differences in common carotid CAT in children with elevated BMI as compared to children with normal BMI, irrespective of age, sex, blood pressure, and Tanner stage. NIVE had previously been shown to detect decreased vascular elasticity in adults with aging, and in men as compared to women [16]. While NIVE has been proven reliable and reproducible in adults [16], and of clinical relevance to characterize atherosclerotic plaques [17, 18], this is the first time it has been studied in great detail in children.

Several studies in the literature have tried to evaluate the complex relationship between arterial stiffness and obesity. Recent meta-analyses have shown increased arterial stiffness in obese children and adolescents as compared to non-obese controls [23, 24]. One of these presented moderate evidence of a relationship with PWV [23], while the other showed a strong relationship with both PWV and β-stiffness index [24]. NIVE

Table 3 Adjusted and unadjusted ANOVA analysis comparing the 6 outcomes between the two groups of children with normal and elevated BMI

	Normal BMI group ($n = 60$)		Elevated BMI group ($n = 60$)			Adjusted mean differences			
	Mean	STD	Mean	STD	*p* value	Mean	95% CI		*p* value
CAS (%)	6.108	1.786	5.722	1.862	0.25	−0.230	−1.336	0.876	0.58
CAT (mm)	0.516	0.176	0.675	0.243	< 0.001	0.163	0.033	0.292	< 0.001*
CAS/CAT	13.348	6.467	9.540	4.814	< 0.001	−4.200	−7.670	−0.729	0.001*
CLT (mm)	0.981	0.336	0.905	0.341	0.22	−0.097	−0.304	0.109	0.21
Max |SEE| (%)	0.480	0.128	0.528	0.126	0.04	0.024	−0.051	0.099	0.38
IMT (mm)	0.322	0.052	0.357	0.053	< 0.001	0.030	−0.002	0.062	0.013

p values are calculated using Student's *t* test for unadjusted mean differences and multiple linear regression for adjusted means (adjusted for age, gender, Tanner stage, blood pressure, and LDL). To account for multiple comparisons, threshold for statistical significance was set at $p < 0.008$ using the conservative Bonferroni correction; 95% CI is also corrected for Bonferroni

CAS (%), cumulated axial strain; *CAT* (mm), cumulated axial translation; *CAS/CAT*, ratio cumulated axial strain over cumulated axial translation; *CLT* (mm), cumulated lateral translation; *Max |SSE|* (%), maximal shear strain; *IMT*, intima-media thickness

*Considered statistically significant using Bonferroni correction

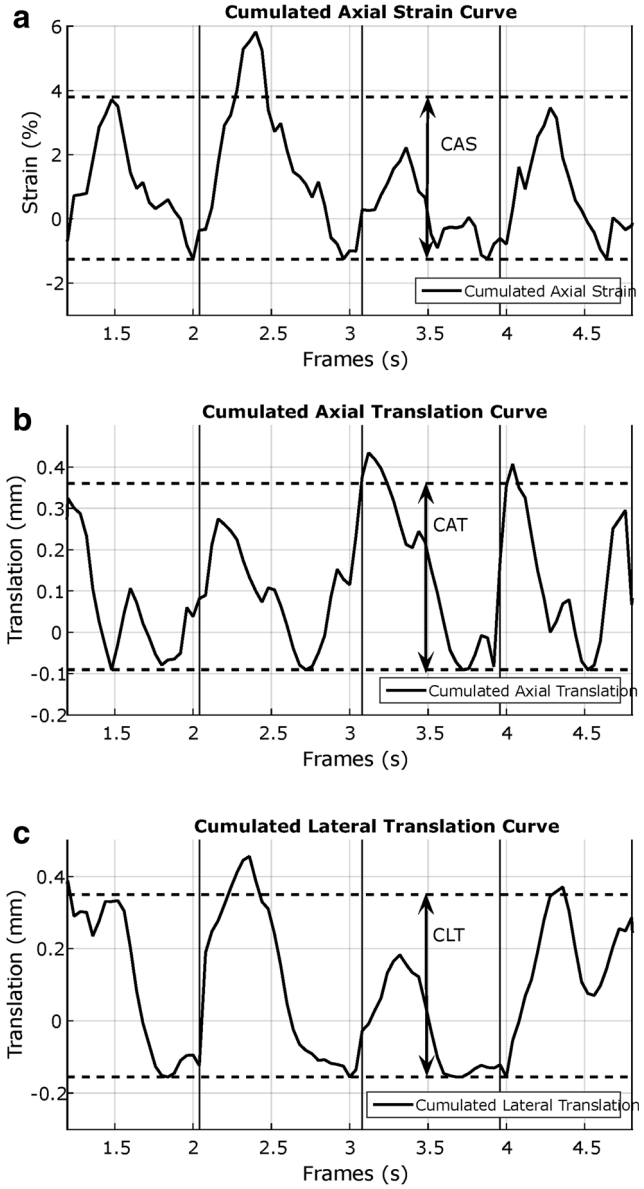

Fig. 3 **a** Graph showing axial strain curves provided by the spatially averaged strain within the segmented area of the carotid artery from every elastogram during systole and diastole. Four cardiac cycles are displayed in this example. The curve represents the cumulated axial strain (CAS) computed between two successive radiofrequency images. The parameter CAS indicates the magnitude of the cumulated strain averaged over all cycles. A negative value for strain indicates vascular tissue compression and hence luminal enlargement (systole), whereas a positive value corresponds to vascular tissue relaxation and hence luminal diameter reduction (diastole). **b** Graph of the cumulated axial translation (CAT) or displacement of the vessel wall. The parameter CAT corresponds to the magnitude of the cumulated translation averaged over all cycles. **c** Same as above, for instantaneous and cumulated lateral translation (CLT)

demonstrated biomechanical differences in arterial function in children with elevated BMI as compared to those with normal BMI. In fact, NIVE could be a potential surrogate for PWV, as it analyzes movement in subsegments of the arterial wall itself. This has been demonstrated in the study of the feasibility of pulse wave imaging in the adult carotid artery [25]. NIVE looks at the elasticity and IMT at the same time.

NIVE reflects the fact that the arterial wall deforms proportionally to pulse pressure during systole and diastole, due to the cyclical driving force inducing wall compression and dilatation. Intuitively, with an increase in blood pressure, the strain magnitude should increase. The maximal shear strain has been shown in adults to assess plaque stability [26]. In children, we found a significantly higher Max |SSE| in the elevated BMI group. This difference did not prevail, however, after adjusting for age and blood pressure. This finding is not surprising, given the central role of blood pressure in shear strain generation. It is in agreement with the factors that led to the recommendations for standardization of the assessment of subclinical atherosclerosis in children, namely, taking blood pressure into account in the interpretation of elasticity and IMT values [27].

After controlling for blood pressure (both systolic and diastolic were higher in the elevated BMI group of our cohort), and using Bonferroni correction, CAT remained significantly higher in children with elevated BMI as compared to those with normal BMI (Table 3). CAT reflects the range of variation in axial translation of the artery as the vessel wall deforms with the cardiac cycle and the lumen size changes accordingly. Moreover, the strain per unit translation (CAS/CAT) was also significantly higher in the normal BMI group even though CAS did not differ between groups. Lower CAS/CAT ratio in the elevated BMI group reflects stiffer arteries deforming less for a similar translation attributed to the pulse pressure. It is proposed as an additional NIVE parameter because it is easier to interpret than CAT alone. The fact that CAS did not differ between groups may be related to the compensatory higher axial motion of the stiffer wall. NIVE results thus indicate certain differences in the mechanical properties of the vessel wall in children with elevated BMI, confirming previous findings of subclinical arteriosclerosis in obese children and adolescents [3, 4], a phenomenon not explained by blood pressure alone.

Elevated IMT is associated with obesity in children [28–30]. IMT measurement techniques in the pediatric population generally rely on B-mode ultrasound and RF echotracking–based ultrasound, using manual or automated/semi-automated techniques. IMT measurements obtained with NIVE segmentation algorithms represent an average value over the entire cardiac cycle and vessel segment. These algorithms include maximum likelihood and iterative methods of exploration selection, based on RF probability distribution data defining image speckle. As with other techniques [28–30], IMT measured by NIVE in our cohort was significantly higher in the elevated BMI group. After Bonferroni correction, however, this difference was no longer significant; notably, Bonferroni represents a conservative approach and is

prone to produce a higher false negative result. Weberruß et al did not find a relationship between BMI and IMT using a semi-automated B-mode technique [31]. This could be related to the poor correlation within the IMT measurement techniques as our results show. Our IMT measurements using NIVE were also lower than the RF echotracking curves published in the literature (mean of 0.4 mm for 15-year-old boys, according to Engelen et al [32]). This could be attributed to the mathematical calculations of IMT inherent in these algorithms, or perhaps to differences in age and sex, as our cohort was children of both sexes, 10–13 years old.

There were several limitations to our study. First, all children in the cohort had an obese parent, introducing potential bias. Prospective studies are therefore needed to test the validity and reproducibility of our results. Second, as there were many covariables, and as a conservative statistical approach is to be used, a larger sample is required to evaluate CAS and Max |SSE| as potential markers. Third, the technique we used to obtain IMT should be compared to other techniques to validate its accuracy; we did not use electrocardiogram-guided measurements or different insonation angles [9]. Lastly, calculation of interobserver variability showed a good to fair agreement for most NIVE-derived measures while one parameter (CAS) had a weak agreement. In general, the ICC values were in the range of agreement found for IMT measurement in children [12].

Conclusion

Childhood overweight and obesity have been on the rise in recent decades and are a known risk factor for atherosclerosis and cardiovascular disease in adulthood. Discernible differences in cumulated axial translation and strain per unit translation were detectable with NIVE when comparing children of normal and elevated BMI. NIVE is thus a promising non-invasive technique that could be useful in monitoring two identified radiological markers of early subclinical atherosclerosis in the follow-up of children with obesity and cardiovascular risk factors.

Acknowledgements The authors are grateful to Danielle Buch, medical writer, for critical revision and substantive editing of the entire manuscript, also including drafting of Abstract.

Funding This study was partially funded by NSERC CHRP 462240-14, CIHR CPG-134748.

Compliance with ethical standards

Guarantor The scientific guarantor of this publication is Dr. Josee Dubois.

Conflict of interest The authors of this manuscript declare no relationships with any companies whose products or services may be related to the subject matter of the article.

Statistics and biometry Mr. Thierry Ducruet, CHU Sainte-Justine, kindly provided statistical advice for this manuscript.

Informed consent Written informed consent was obtained from all subjects (patients) in this study.

Ethical approval Institutional Review Board approval was obtained.
Ste-Justine Hospital Ethics Review Board
Quebec Lung and Heart Institute

Study subjects or cohorts overlap Some study subjects or cohorts have been previously reported in the QUALITY study (Quebec Adipose and Lifestyle InvesTigation in Youth) and in the article *Carotid artery intima-media thickness measurement in children with normal and increased body mass index: A comparison of three techniques* (Pediatric Radiology, August 2018, vol 48, issue 8, pages 1073-1079.

Methodology
- prospective
- experimental
- performed at one institution

References

1. McGill HC Jr, McMahan CA, Zieske AW et al (2000) Associations of coronary heart disease risk factors with the intermediate lesion of atherosclerosis in youth. The Pathobiological Determinants of Atherosclerosis in Youth (PDAY) Research Group. Arterioscler Thromb Vasc Biol 20(8):1998–2004
2. Baker JL, Olsen LW, Sørensen TI (2007) Childhood body-mass index and the risk of coronary heart disease in adulthood. N Engl J Med 357(23):2329–2337
3. Raitakari OT, Juonala M, Rönnemaa T et al (2008) Cohort profile: the cardiovascular risk in Young Finns Study. Int J Epidemiol 37(6): 1220–1226
4. Silva LR, Stefanello JM, Pizzi J, Timossi LS, Leite N (2012) Atherosclerosis subclinical and inflammatory markers in obese and nonobese children and adolescents. Rev Bras Epidemiol 15(4):804–816
5. Anderson TJ (2006) Arterial stiffness or endothelial dysfunction as a surrogate marker of vascular risk. Can J Cardiol 22(Suppl. B): 72B–80B
6. McGill HC Jr, McMahan CA, Zieske AW et al (2000) Association of coronary heart disease risk factors with microscopic qualities of coronary atherosclerosis in youth. Circulation 102(4):374–379
7. De Korte CL, Hansen HH, van der Steen AF (2011) Vascular ultrasound for atherosclerosis imaging. Interface Focus 1(4):565–575
8. Lim HS, Lip GY (2008) Arterial stiffness: beyond pulse wave velocity and its measurement. J Hum Hypertens 22(10):656–658
9. Selamet Tierney ES, Gauvreau K, Jaff MR et al (2015) Carotid artery intima-media thickness measurements in the youth: reproducibility and technical considerations. J Am Soc Echocardiogr 28(3):309–316
10. Dalla Pozza R, Ehringer-Schetitska D, Fritsch P et al (2015) Intima media thickness measurement in children: a statement from the

Association for European Paediatric Cardiology (AEPC) Working Group on cardiovascular prevention endorsed by the Association for European Paediatric Cardiology. Atherosclerosis 238(2):380–387
11. Touboul PJ, Hennerici MG, Meairs S et al (2012) Mannheim carotid intima-media thickness and plaque consensus (2004-2006-2011): an update on behalf of the advisory board of the 3rd and 4th watching the risk symposium 13th and 15th European Stroke Conferences, Mannheim, Germany, 2004, and Brussels, Belgium, 2011. Cerebrovasc Dis 34(4):290–296
12. El Jalbout R, Cloutier G, Cardinal MR et al (2018) Carotid artery intima-media thickness measurement in children with normal and increased body mass index: a comparison of three techniques. Pediatr Radiol 48(8):1073–1079
13. Reusz GS, Cseprekal O, Temmar M et al (2010) Reference values of pulse wave velocity in healthy children and teenagers. Hypertension 56(2):217–224
14. Mercure E, Cloutier G, Schmitt C, Maurice RL (2008) Performance evaluation of different implementations of the Lagrangian speckle model estimator for non-invasive vascular ultrasound elastography. Med Phys 35(7):3116–3126
15. Mercure E, Destrempes F, Roy Cardinal MH et al (2014) A local angle compensation method based on kinematics constraints for non-invasive vascular axial strain computations on human carotid arteries. Comput Med Imaging Graph 38(2):123–136
16. Maurice RL, Soulez G, Giroux MF, Cloutier G (2008) Non-invasive vascular elastography for carotid artery characterization on subjects without previous history of atherosclerosis. Med Phys 35(8):3436–3443
17. Roy Cardinal MH, Heusinkveld MHG, Qin Z et al (2017) Carotid artery plaque vulnerability assessment using noninvasive ultrasound elastography: validation with MRI. AJR Am J Roentgenol 209(1):142–151
18. Cloutier G, Cardinal MR, Ju Y, Giroux MF, Lanthier S, Soulez G (2018) Carotid plaque vulnerability assessment using ultrasound elastography and echogenicity analysis. AJR Am J Roentgenol 211(4):847–855
19. Lambert M, Van Hulst A, O'Loughlin J et al (2012) Cohort profile: the Quebec adipose and lifestyle investigation in youth cohort. Int J Epidemiol 41(6):1533–1544
20. Paradis G, Lambert M, O'Loughlin J et al (2003) The Québec child and adolescent health and social survey: design and methods of a cardiovascular risk factor survey for youth. Can J Cardiol 19(5):523–531
21. Destrempes F, Meunier J, Giroux MF, Soulez G, Cloutier G (2009) Segmentation in ultrasonic B-mode images of healthy carotid arteries using mixtures of Nakagami distributions and stochastic optimization. IEEE Trans Med Imaging 28(2):215–229
22. Destrempes F, Meunier J, Giroux MF, Soulez G, Cloutier G (2011) Segmentation of plaques in sequences of ultrasonic B-mode images of carotid arteries based on motion estimation and a Bayesian model. IEEE Trans Biomed Eng 58(8):2202–2211
23. Hudson LD, Rapala A, Khan T, Williams B, Viner RM (2015) Evidence for contemporary arterial stiffening in obese children and adolescents using pulse wave velocity: a systematic review and meta-analysis. Atherosclerosis 241(2):376–386
24. Cote AT, Phillips AA, Harris KC et al (2015) Obesity and arterial stiffness in children: systematic review and meta-analysis. Arterioscler Thromb Vasc Biol 35(4):1038–1044
25. Luo J, Li RX, Konofagou EE (2012) Pulse wave imaging of the human carotid artery: an in vivo feasibility study. IEEE Trans Ultrason Ferroelectr Freq Control 59(1):174–181
26. Naim C, Cloutier G, Mercure E et al (2013) Characterisation of carotid plaques with ultrasound elastography: feasibility and correlation with high-resolution magnetic resonance imaging. Eur Radiol 23(7):2030–2041
27. Urbina EM, Williams RV, Alpert BS et al (2009) Noninvasive assessment of subclinical atherosclerosis in children and adolescents: recommendations for standard assessment for clinical research: a scientific statement from the American Heart Association. Hypertension 54(5):919–950
28. Ozcetin M, Celikyay ZR, Celik A, Yilmaz R, Yerli Y, Erkorkmaz U (2012) The importance of carotid artery stiffness and increased intima-media thickness in obese children. S Afr Med J 102(5):295–299
29. Johnson HM, Douglas PS, Srinivasan SR et al (2007) Predictors of carotid intima-media thickness progression in young adults: the Bogalusa Heart Study. Stroke 38(3):900–905
30. Lorenz MW, Markus HS, Bots ML, Rosvall M, Sitzer M (2007) Prediction of clinical cardiovascular events with carotid intima-media thickness: a systemic review and meta-analysis. Circulation 115(4):459–467
31. Weberruß H, Pirzer R, Böhm B, Dalla Pozza R, Netz H, Oberhoffer R (2016) Intima-media thickness and arterial function in obese and non-obese children. BMC Obes 3:2
32. Engelen L, Ferreira I, Stehouwer CD, Boutouyrie P, Laurent S (2013) Reference values for arterial measurements collaboration. Reference intervals for common carotid intima-media thickness measured with echotracking: relation with risk factors. Eur Heart J 34(30):2368–2380